A Particle Swarm Optimization–based heuristic to optimize the configuration of artificial barriers for the mitigation of lava flow risk

Veronica Centorrino[a], Giuseppe Bilotta[a], Annalisa Cappello[a,*], Gaetana Ganci[a], Claudia Corradino[a] and Ciro Del Negro[a]

[a]*Istituto Nazionale di Geofisica e Vulcanologia, Osservatorio Etneo, Piazza Roma 2, Catania 95125, Italy*

ARTICLE INFO

Keywords:
Particle Swarm Optimization
Artificial barrier
Lava flow risk
Numerical simulations
MAGFLOW

Abstract

Lava flows are recurring and widespread hazards that affect areas around active volcanoes, having the potential to cause significant social and economic loss. The ongoing demographic congestion around volcanoes increases the potential risk and leads to a growing demand for faster and more accurate systems to safeguard the population. The main mitigation action for slowing down and possibly diverting lava flows is the building of artificial barriers, that can limit their destructive effects and reduce losses. Here we present a Particle Swarm Optimization algorithm for the configuration of artificial barriers, in terms of location and geometric features. The goal is minimizing the lava flow impact based on the spatial distribution of exposed elements, using the physics-based MAGFLOW model to run the lava flow scenarios for each barrier configuration. Our algorithm has been tested on Etna (Italy), showing how it can effectively safeguard the threatened areas, diverting lava away from them.

1. Introduction

Volcanic risk can be described as the loss (of lives and properties) due to hazardous phenomena in a certain (volcanic) area over specific periods, where the consequences are determined by the exposed elements and their level of vulnerability to hazards (Fournier D'Albe, 1979). From a mathematical point of view, risk can be computed as the product of hazard, vulnerability and exposure, where hazard is a measure of the probability of occurrence of the destructive event, vulnerability is a measure of how strongly the areas are affected by the event (ranging continuously from 0 for "no loss" to 1 for "total loss"), and exposure is a quantification of the value of the affected areas.

In the case of lava flow risk, vulnerability is generally assumed to take only the extreme value of 1 (total loss), since lava flows commonly cause complete devastation through properties or towns (Thierry et al., 2008; Favalli et al., 2009; Pedrazzi et al., 2014). Consequently, the risk from lava flow inundation can be estimated simply as the product of hazard (the probability of a lava flow reaching a particular area) and exposure, so that risk mitigation can be achieved by affecting the hazard, i.e. altering the probability of invasion, which requires a way to influence the progress of a lava flow.

The idea of slowing and diverting lava flows with the use of artificial structures for the mitigation of its risk thus arises from simple physical considerations. The emplacement of lava flows is essentially controlled by the effusion rate, the rheology of the lava, and the topography. Since the effusion rate and the rheology of the fluid are outside of our control, the main viable tool to influence a lava flow remains our possibility to impact the topography, to divert the flow. The topography influences the emplacement both directly, by offering preferential directions to the flow, and indirectly, by influencing the capability for the flow to develop lava tubes, known to be particularly hazardous due to their thermal insulation that allows the tunneled lava to preserve a high fluidity for longer times, and thus to cover higher distances before cooling off and slowing down (Walker et al., 1973; Calvari and Pinkerton, 1999).

When lava is diverted out of its natural channel, the flow front is deprived of back-thrust and is not able to advance any longer, generating a new front from the diversion point. If only a partial lava diversion is achieved, the flow front stops due to the reduction of the back-thrust, and none of the two flows resulting from the partial diversion can travel as far as the initial one. In both cases, it has been experienced that the use of structures, such as artificial barriers or ditches, to divert lava flows is an effective action for mitigating its risk.

One of the main volcanoes giving the foremost examples of lava flows with significant impact on densely populated areas is Mt Etna (Sicily, Italy, Figure 1a), due to the high frequency of effusive eruptions (Cappello et al., 2013;

*Corresponding author

Del Negro et al., 2013). Here, the building of artificial barriers has been proven to be an effective action for diverting and slowing down the lava flows, as experienced during recent eruptions (e.g. 1983, 1991–1993, 2001, 2002), when earthen barriers were built to control lava flow expansion with varying degrees of success (Colombrita, 1984; Barberi et al., 1993, 2003; Barberi and Carapezza, 2004).

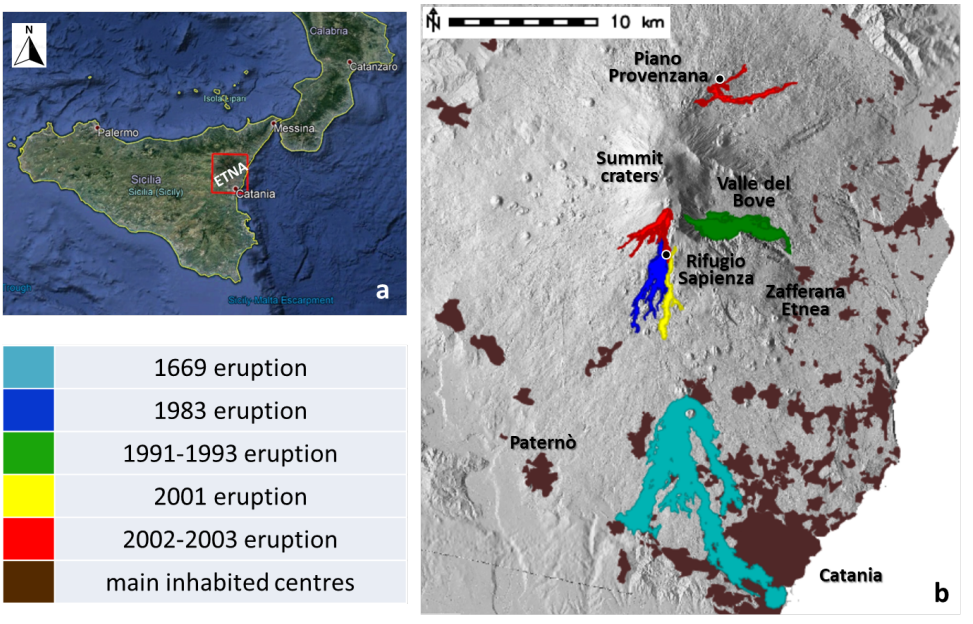

Figure 1: a) Google Earth view of Etna location in Sicily, Italy; b) historical effusive eruptions, during which mitigation action were taken. The main inhabited centres on Etna's flank are also reported.

Providing effective and objective solutions is very challenging, since the best positioning of these artificial constructions depends on many factors, such as the viscosity of the lava, the output rates, the topography of the affected area, the time of intervention and the economic costs for construction. For this reason, the design of the mitigation measures is generally based on the past experience and knowledge of experts, leaving the problem of defining a standard methodology for the construction and location of protection structures still open.

The task of finding optimal intervention strategies for volcanic risk mitigation can be seen as an optimization process, whose goal is to find the "best" configuration of barriers and ditches minimizing both the damage caused by the (diverted) flow and the cost of the intervention itself. As with all optimization processes, the solution can be found by searching through the (abstract) space of potential solutions.

For small spaces, classical exhaustive methods are usually sufficient; but most real-world problems, such as the design of the mitigation measures for volcanic risk, have high complexity, non-linear constraints, interdependencies among variables, and huge solution spaces. This needs the use of a method capable of solving complex optimization problems in real-time.

Metaheuristic algorithms are optimization methods that produce a reasonably good solution in a moderate amount of time and can be used to efficiently solve problems with large number of variables and non-linear objective functions. Thanks to their properties and wide fields of application, in the past two decades, many metaheuristic algorithms have been proposed. Some examples are particle swarm optimisation – PSO (Kennedy and Eberhart, 1995b), genetic algorithms – GA (Holland, 1992), simulated annealing – SA (Kirkpatrick et al., 1983), tabu search – TS (Glover and Marti, 2006), ant colony optimisation – ACO (Dorigo, 1992) and differential evolution – DE (Price et al., 2005). In the literature (see e.g. Gogna and Tayal (2013)) there are different ways to classify metaheuristic algorithms based on characteristics used to differentiate amongst them. They include: nature inspired (e.g. PSO, GA) versus non-nature inspired (e.g. TS); population-based (e.g. PSO, GA) versus single-point search (e.g. TS, SA and local search); iterative (e.g. PSO, SA) versus greedy (e.g. ACO); dynamic (e.g. guided local search) versus static (e.g. PSO) objective function.

Among them, population-based metaheuristics (P-metaheuristics), most of which are inspired by nature, represent

a reasonable solution when the hazardous event to simulate evolves based on local interactions of their constituent parts. They apply the generation and replacement procedure to a family of solutions spread over the search space until the stopping criterion is met. For example, Filippone et al. (2013) presents an application of Parallel Genetic Algorithms for optimizing earth barriers construction to divert a lava flow on Mt Etna and protect the touristic facility of Rifugio Sapienza. Our goal is to combine one of the P-metaheuristics algorithms with the MAGFLOW lava flow model (Del Negro et al., 2008; Cappello et al., 2016), to determine the optimal position and geometric features of more than one structure able to divert the flow in case of an eruption to mitigate lava flows hazard. Among the population-based metaheuristics, we decided to use the PSO algorithm since its implementation perfectly fits the definition of a barrier and its geometric parts, the possibility to use more than one structure, forming a "particle", and it presents a good coupling with MAGFLOW too. Our choice relies also on computational time, in which the time necessary to run the MAGFLOW simulations play a huge part, since the PSO algorithm has proven to converge rapidly in comparison with other models (see e.g. El-Ghandour and Elbeltagi (2018) in which it is compared with GA, ACO, MA and the modified shuffled frog leaping algorithm, SFLA).

Our PSO algorithm minimizes the impact of lava flows based on the spatial distribution of exposed elements and using the numerical MAGFLOW model to run the eruptive scenarios associated with each barrier configuration. Here it has been applied and validated using a possible lava flow erupted from a vent located on the southeastern flank of Mt. Etna. The geological map of the Mount Etna (Branca et al., 2011) shows that a number of eruptions were produced from vents located in this same area. More recent eruptions, occurred in 1634 and 1792, were characterized by long duration (540 and 340 days, respectively) and high volumes of lava (about 150 Mm^3 and 62 Mm^3, respectively), whose flows arrived to destroy some villages (Behncke et al., 2005). Therefore the opening of future eruptive vents in the southeastern flank of the volcano presents a very high potential risk for the destructive impact that the new flows could have on the near urbanized areas (Del Negro et al., 2013, 2019).

We found barrier configurations that have the potential to completely protect the villages threatened by lava, showing how this methodology is effectively able to divert the flow, safeguarding the inhabited areas.

The paper is organized as follows. In Section 2, we present a brief review of the mitigation actions against historical eruptions at Mt. Etna. In Section 3, we illustrate the main features of the PSO algorithm, while in Section 4, we describe the main characteristics of the implemented algorithm: we define the search space and the target function, the constraints for the barrier placement, the way the particle system is initialized, and how the swarm evolves. In Section 5, we provide a numerical example to illustrate the effectiveness of the proposed mitigation strategy. In Section 6, we discuss the achieved results. Section 7 concludes this paper with a summary of our results and some possible future developments. Finally, in Appendix A we describe the mathematical law used to enforce barrier position constraints, while in Appendix B we present the results of other two runs for the numerical example provided in Section 5.

2. Mitigation actions against historical effusive eruptions at Mt. Etna

The first attempt to control a lava flow dates back to 1669 (Figure 1b), during the most devastating historic eruption of Mt Etna (Barberi et al., 1993). When the lava was proceeding into the city of Catania, a group of frightened citizens tried to protect themselves opening a breach on a levee of the flow to change its advance direction. Unfortunately, this initially promising attempt was stopped by hundreds of furious residents of the nearby Misterbianco village, who feared that their houses could be destroyed by the diverted lava flow.

After 1669, mitigation measures trying to divert lava flows at Mt Etna were blocked mainly due to legal disputes related to the fact that the flow diverted to defend one city could threaten another one.

It was only in 1983 that the Italian government authorized a direct intervention, constructing an artificial opening of a breach on the levee of a channelized flow to divert the lava from its natural bed into an artificial channel, excavated parallel to the natural one. This area was a public property, so no disagreement with private owners arose. The break opened by an explosion on the levee was relatively small and diverted into the artificial channel only 20-30% of the lava, while the remaining 70-80% continued to flow into the natural one. As an indirect consequence of the explosion, a very substantial deviation of the flow out of its natural channel was achieved and, despite only a short partial diversion was obtained, the desired result was achieved since most of the lava out flowed, due to the obstruction of a nearby lava tube. This intervention was only a partial success, but demonstrated that man was effectively able to control the expansion of a lava flow.

After the 1983 eruption, Mt Etna had an intense eruptive activity. A particular significant case is the 1991–1993 eruption (Figure 1b), because of the several actions carried out to protect the village of Zafferana Etnea from being

invaded by the lava. The strategy adopted in this situation was an improvement of the methods used during the 1983 lava deviation obtaining a total diversion of the flow. The measures to defend Zafferana included the building of four lava containment earth barriers and several attempts at plugging the lava tube. Downhill, the earth barriers, oriented orthogonally to the direction of the flow, slowed the front propagation down for a few weeks although they were not able to fully stop it. Since lava was overflowing on the earth barriers the Civil Protection authorities had to carry out a drastic lava flow deviation near the vent. Finally, the flow was diverted into an artificial channel by blasting the wall separating it from the natural channel and obstructing downstream the natural tunnel (Barberi et al., 1993). Overall, during this event, 13 earth barriers were built, providing a positive experience at Mt Etna to protect towns from lava flows, even if some legal questions had not been fully solved yet. However, from the detailed reconstruction of lava tube formation and flow evolution of this eruption and by comparison with other historic eruptions of Mt Etna, Calvari and Pinkerton (Calvari and Pinkerton, 1998) showed that without the successful diversion of May 1992, the lava would have overcome Zafferana Etnea and continued beyond.

An intervention similar to the one adopted in 1992 was planned to deviate the flow during the 2001 eruption that threatened the tourist facilities in the Rifugio Sapienza area (Figure 1b). It included the construction of both lateral earth barriers to push the flow toward existing large holes and orthogonal bars to increase the holding capacity of the depressions. Moreover, a possible evacuation of the nearby villages was also planned. Because of the decreasing of the effusion rate, the plan was only partially executed and just 13 barriers were built up to protect the area, initially delaying the advance of the flows and then diverting it toward south-east, away from the facilities (Barberi and Carapezza, 2004).

Finally, structures to divert lava flows were planned during the 2002–2003 eruption of Mt Etna, which produced two lava flows (Figure 1b) partially covering the tourist facilities of Piano Provenzana (on the northern side of the volcano) and threatening Rifugio Sapienza (on the southern flank)(Andronico et al., 2005). In this case, a great effort was devoted to the construction of six earth barriers, in accordance with the local authorities, including the Etna Volcanological Park. These actions contributed to mitigate the impact of the lava flows advance considering that on November 24 the flows directed toward the south were deviated away from the touristic facilities of Rifugio Sapienza. Unfortunately, on December 16 the lava overflowed from the barrier destroying two buildings and cutting the "SP92" road before stopping soon after (Scifoni et al., 2010).

3. Particle Swarm Optimization

The building of artificial barriers at Etna volcano has been an effective action for diverting and slowing down different lava flows. However the decision of the construction site was mainly based on expert advice, leaving the problem of defining a standard methodology for the location of protection structures to mitigate volcanic risk still open. For this reason, we developed an automatic algorithm based on particle swarm optimization and the MAGFLOW model, which aims at finding the best configuration of artificial barriers, in terms of location and geometric features. Before describing the main characteristics of our algorithm, we briefly present the particle swarm optimization paradigm.

Particle swarm optimization (PSO, Kennedy and Eberhart (1995a,b)) is a stochastic optimization algorithm based on the simulation of the behavior of socially organized populations in nature, such as bird flocks, fish schools, and animal herds. One of the main advantages of PSO is that it can be applied to non-differentiable, non-linear problems with a very large search space (e.g. high number of dimensions) with good efficiency.

The idea is that, to find the minimum of a real-valued function f over a domain $D \subset \mathbb{R}^n$, we can "sample" the function by computing $f(x_i)$ for a given set of points x_i in D, and then *move* the points x_i with some velocity v_i towards the positions that achieved the lowest values. This results in a *swarm*

$$S = \{x_1, x_2, \dots, x_N\},$$

of N *particles* that iteratively move within the *search space* D, converging towards the point where f achieves its minimum value.

Putting it in a mathematical framework, let us denote by $x_i(t) \in D$ the position of the i-th particle of S at iteration t, and by $v_i(t) \in \mathbb{R}^n$ its velocity, where n is the number of components of each particle. Each particle has a "memory" of the best position $b_i(t)$ it has occupied so far, i.e.

$$b_i(t) = \arg\min_{\tau} f(x_i(\tau)), \text{ with } 0 \le \tau \le t,$$

and the swarm as a whole has knowledge of the best position $b_g(t)$ occupied so far by any particle, i.e.

$$b_g(t) = \arg\min_{i} f(b_i(t)), \text{ with } 1 \le i \le N.$$

The initial values for the position $x_i(0)$ and $v_i(0)$ are chosen randomly, and initially $b_i(0) = x_i(0)$. At every iteration, the velocity of each particle is updated considering the previous velocity, a *cognitive factor* based on the particle's best position, and a *social factor* based on the swarm's best position. Formally, given fixed weights ω, c_1, c_2 and random values $R_1(t), R_2(t) \in [0, 1]$, the velocity and position update formulas can be written, following the improvement proposed by Shi and Eberhart (Shi and Eberhart, 1998):

$$\begin{aligned} v_i(t+1) &= \omega v_i(t) + c_1 R_1(t) \left(b_i(t) - x_i(t)\right) + c_2 R_2(t) \left(b_g(t) - x_i(t)\right), \\ x_i(t+1) &= x_i(t) + v_i(t), \end{aligned} \tag{1}$$

for $i = 1, 2, \ldots, N$. The coefficient ω is know as the *inertia weight* and indicates a tendency of each particle to continue in the direction it was already moving; c_1 is the *cognitive parameter* and it controls the weight with which particles are attracted to their best known position, while c_2 is the *social parameter* and it controls the weight with which particles are attracted to the best known position of the entire swarm.

4. Mitigation of lava flow risk using PSO and MAGFLOW

To apply the PSO algorithm for the mitigation of lava flow risk, we need to map the physical problem onto mathematical concepts in such a way that the evaluation of the target function f relies on the lava flow emplacement simulations done with the numerical MAGFLOW model, and the motion of the particles respects the constraints due to the considered physical problems.

4.1. Definition of the search space and target function

The search space is defined by the possible locations and geometric characteristics for the barriers, and the target function to be minimized is the impact of the eruptive scenario.

We assume that barriers have a "winged" configuration, so that a single barrier can be defined by six values: the *easting* and *northing* of the central point, the *length* of the two arms, the *height* of the barrier (with a negative height indicating a ditch) and the two angles, *langle* and *rangle*, that the arms form with respect to the north/south and east/west direction (Figure 2).

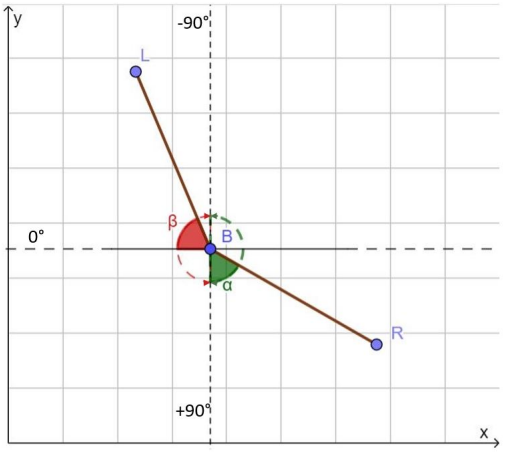

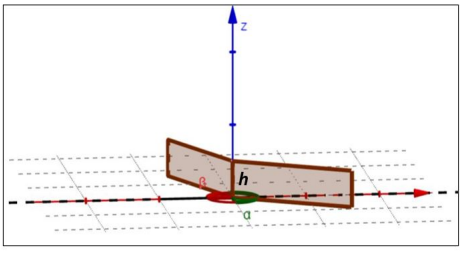

Figure	Configuration
B (easting, northing)	Barrier position
α	Rangle
β	Langle
BR = BL	Length
h	Height

Figure 2: Top (left) and lateral (top right) view of the "winged" configuration of barriers. The table reports the 6 parameters that characterize each barrier B.

We assume that in the case of intervention, multiple barriers may need to be built, so a single *particle* in our swarm is a collection of a (fixed) number of barriers: if there are B barriers, the dimensionality of our problem is then $6B$, since each particle is defined by the 6 parameters of each of the barriers that compose it. The (fixed) number of barriers represents the maximum number that can be used and its choice depends on the feasibility in terms of the economic possibilities and timing. Note that the *position* of a particle is an abstract concept in this case, since it includes the *physical* position, but also the angles, length and height of each of its barriers.

Our target function is the potential loss associated with a eruptive scenario. As a simplification in this initial stage of development, we define the loss by simply estimating the amount of inhabited areas reached by the lava flow. The computation of the target function requires an assessment of the impact of the barriers on the lava flow emplacement, that we compute using MAGFLOW, a Cellular Automaton model for lava flow simulations developed at INGV, Sezione di Catania (Cappello et al., 2016; Bilotta et al., 2012, 2019).

In MAGFLOW, the area of interest for the simulation is decomposed into a regular grid of square cells with associated information including: the terrain elevation, the amount of solid and liquid lava present in the cell, and its temperature. The evolution function of the automaton is based on a steady-state solution of the Navier–Stokes equation for Bingham fluids, coupled with a simplified physical model for the thermal evolution of the flowing lava (Vicari et al., 2007). MAGFLOW has proven to be successful both to reproduce past events with well-known characteristics and to predict the paths of lava flows in real time, for example during the Mt Etna eruptions of 2004 (Del Negro et al., 2008), 2006 (Vicari et al., 2009; Hérault et al., 2009), 2008 (Bonaccorso et al., 2011; Ganci et al., 2012) and 2011 (Vicari et al., 2011). Inputs to MAGFLOW are the digital topography of the area of interest (taken from a DEM, Digitial Elevation Model), the location of the vent(s), and the mass flux rate as a function of time. Optionally, it is also possible to specify the location and geometry of an arbitrary number of barriers and ditches, that are realized by adding or removing a corresponding amount of height from the DEM in the affected areas. The output of the MAGFLOW model is a sequence of snapshots of the spatio-temporal evolution of the emplacement, taken at fixed intervals (chosen by the user). In our case, we only look at the final emplacement.

To integrate MAGFLOW with our PSO algorithm, we also include for each cell the information about whether the cell is inside an inhabited center or not. For each particle in the swarm, i.e. for each set of barriers, we run a MAGFLOW simulation, and the target function for that particle (i.e. score of the barrier configuration) is computed by counting the number of township cells with lava. The objective of the PSO is then to minimize this value.

The main steps of the algorithm can be summarized as follows:

pre-flight: (a) run a MAGFLOW simulation without any barriers; (b) calculation of the score, set as *best score*;

particle system initialization: (a) initialization of a swarm; (b) run MAGFLOW simulations with the barrier configuration of each particle in the swarm; (c) calculation of the score; (d) comparison with the *best score* and replacement if lower;

swarm evolution: (a) definition of a new configuration; (b) run MAGFLOW simulations with the new configuration; (c) calculation of the score; (d) comparison with the *best score* and replacement if lower.

The sequence of the swarm evolution phase is repeated until convergence is reached.

4.2. Quantization of the search space

To help reduce the search space, all of the dimensions that control the barrier configuration, and thus the particle position and velocity in the abstract space, are quantized, in the sense that they do not vary continuously, but only in multiples of a discrete step. The size of this step is a user-controlled parameter, and can be varied for different dimensions. The default values (used in the examples presented here) are 10 meters for the position, 1 meter for the length, 5 meters for the height and 10° (sexagesimal) for the angles.

4.3. Barrier placement constraints

In a straightforward application of the PSO, the search space with our choice of particles would have not only a high dimensionality, but also a very large span, especially for the choice of the position of the barrier vertex. Indeed, a naive choice for the boundaries of the easting and northing coordinates for the barriers could be the bounding box of the original lava flow emplacement, even though in most of these locations barriers would not interact with the lava flow at all (see e.g. Figure 3). Moreover, most of these positions would be equivalent (all have the same score), leading to a very slow convergence.

A possible solution is to add a constraint on the barrier location, to ensure it actually interacts with the lava flow, for example by requiring that the barrier vertex is confined to be inside the lava flow. However, since the barriers themselves alter the flow emplacement, this is impossible to achieve consistently with multiple barriers, due to the way they affect each others' domain. To work around the issue, we let the barrier location change freely, but we keep track of the lava flow point closest to the barrier placement. This information is then used to correct the barrier position if moved too far away from the flow.

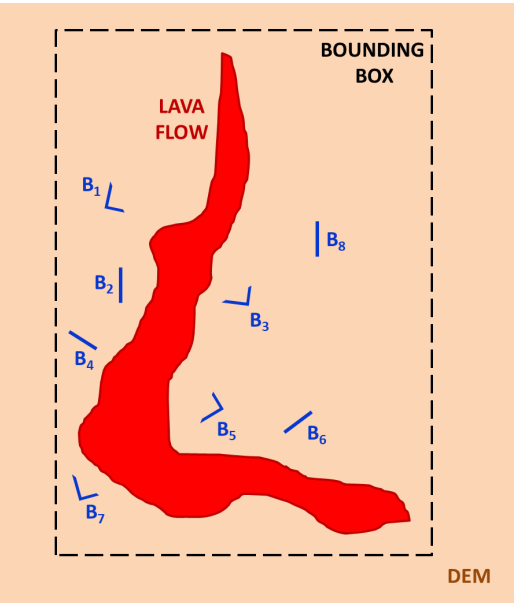

Figure 3: Example of barriers ($B_1, B_2, ..., B_8$) of a particle (in blue) having the bounding box (dashed black area) of the original lava flow (in red) as search space, but not interacting with it.

Further constraints are posed on barrier placement to avoid unrealistic situations. In particular, we require that barriers do not get too close to the vent(s), and that they should not be located inside a town. Appendix A details how these constraints are enforced.

4.4. Particle system initialization

The first step of our PSO algorithm is the initialization of the particles with random positions and velocities. Due to the constraints on the barrier positions, we first run MAGFLOW assuming no barriers are present. This gives us an upper bound to the "best score" for the algorithm, and a reference emplacement of the lava flow to guide the initial placement of the barriers.

The particles for the swarm are then generated. The procedure we will describe momentarily to generate the initial positions and velocities of the particles was designed to solve the mapping issue between corresponding barriers of the different particles.

To illustrate the issue, assume for simplicity that each particle in the swarm is composed of two barriers ($B = 2$). Then particle i will have coordinates

$$(B_i^1, B_i^2) = (e_i^1, n_i^1, \alpha_i^1, \beta_i^1, l_i^1, h_i^1, e_i^2, n_i^2, \alpha_i^2, \beta_i^2, l_i^2, h_i^2)$$

(easting, northing, right and left angle, length and height for the first barrier and for the second barrier, in order). Now consider a second particle j with coordinates

$$(B_j^1, B_j^2) = (e_j^1, n_j^1, \alpha_j^1, \beta_j^1, l_j^1, h_j^1, e_j^2, n_j^2, \alpha_j^2, \beta_j^2, l_j^2, h_j^2)$$

and assume that the barriers of particle i and j are as in Figure 4, the first barrier of the first particle, B_i^1 is closer to the second barrier of the second particle, B_j^2, while the second barrier of the first particle, B_i^2, is closer to the first barrier of the second particle, B_j^1. In extreme situations, the two particles could represent identical configurations, but with swapped barrier order: while the PSO algorithm assumes a component-by-component mapping between particles, in these cases some kind of transformation would be required to improve convergence.

To avoid these situations and ensure a correct component mapping, we generate particles iteratively as perturbations of an initial configuration. Specifically, we first generate the first particle of the swarm by generating random position, velocities, angles, length and height for each of the particle barriers. The only constraint in this case is that the positions of the barriers are not too close to the vent, and not too close to the other barriers being generated.

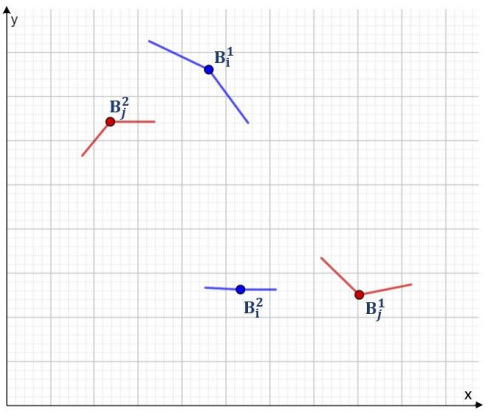

Figure 4: Example of two particles ((B_i^1, B_i^2) in blue and (B_j^1, B_j^2) in red) where the natural mapping between barriers does not match the order, since the first barrier of the first particle is closer to the second barrier of the second particle, and the second barrier of the first particle is closer to the first barrier of the second particle.

For each of the other particles, we only generate the first barrier randomly: the position of all other barriers in the particle is obtained by shifting the corresponding barrier of the first particle by the distance vector between the first barrier of the first particle and the first barrier of the particle being generated (Figure 5).

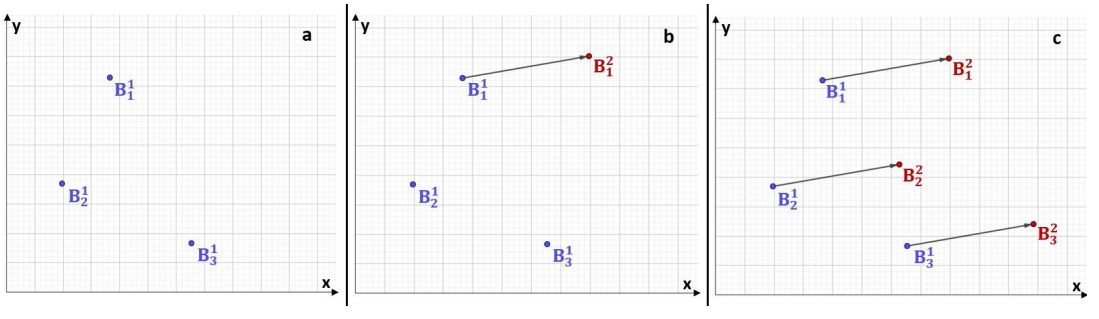

Figure 5: Example of swarm initialization. The barriers of the first particle are randomly generated first (a). For each other particle, a random barrier is generated (b) and the offset of this barrier to the first barrier of the first particle is used to generate the other barriers of this particle (c).

After all particles are generated, their positions are adjusted to ensure that the other constraints on the position are satisfied, moving them closer to the flow and outside of the towns, as necessary. The details about the application of these constraints are illustrated in Appendix A.

4.5. Swarm evolution

The evolutionary step of the swarm can be summarized in the following sequence: we compute the target function for each of the particles in the swarm; if the current score is lower than the previous best score for that particle, the best score (and corresponding configuration) of the particle is saved for reference; if the lowest score among the particles is lower than the previous record, the best score (and corresponding configuration) of the swarm is saved for reference; positions and velocities for each particle are updated according to Equation (1); the physical positions of the barriers of each particle are corrected to take into account the placement constraints, as explained in Appendix A.

The above sequence is repeated until convergence is reached. Convergence is assumed if the best score for the swarm does not improve for a user-settable number of iterations, defaulting to 10.

5. Test case: Barrier configuration for a lava flow on Mt Etna

We validate our PSO–based algorithm to mitigate the risk of a hypothetical lava flowing on the south flank of Mt Etna. We run a simulation without any artificial barriers and a set of possible scenarios using our PSO approach. All simulations have been performed using the GPU version of the MAGFLOW model (Cappello et al., 2016) on a machine equipped with an 8-core Intel Xeon E5-1620v3 CPU running at 3.5GHz, and an NVIDIA GeForce GTX TITAN X (Maxwell architecture) GPU.

The hypothetical lava flow lasts 15 days and is erupted from a vent (UTM-WGS84 coordinates $502737E, 4172403N$) situated on the southeastern east flank of Etna. As effusion rate, we considered a bell-shaped curve (typical of the flank eruptions on Etna), which starts from a null value, reaches the peak of 50 m^3/s after a 1/3 of the eruption time, and then gradually decreases until the end. All simulations were run on a 10 m resolution DEM of Mt. Etna updated to 2007, and adopting the typical physical and rheological properties of the Etnean lava (Bilotta et al., 2012; Del Negro et al., 2013).

For the PSO parameters, we set the inertia weight $\omega = 0.9$ and the cognitive and social parameters $c_1 = c_2 = 2$. The probable number of barriers depends on the economic possibilities and timing, while the number of particles hinges upon the amount of barriers and the computational time. Indeed, there is an indirect correlation between the number of barriers and particles, because the more barriers there are, the more particles should be used to reduce the number of steps needed to explore the configuration space. On the other hand, the number of particles also controls the computational time, which is almost entirely covered by the time necessary to run the MAGFLOW simulations for each configuration. Therefore the number of particles had been chosen as a compromise between the computational time and the number of steps needed. These considerations have led us to choose 64 particles and 9 barriers.

Regarding the barrier size, we settled for 256m and 32m as maximum length and height, respectively. These dimensions are greater than those used in historical precedents. However, in this first phase we decided to make this choice since our main objective was to test our method and validate its effectiveness. Finally, we define the minimum acceptable distance of a barrier from the vent as 2km.

First, the algorithm ran a MAGFLOW simulation without any barrier and calculated its score (Figure 6a). We recall that the objective function counts the area of the towns invaded zones: the score is obtained counting every DEM cell that belongs to a township (i.e. the value of the cell in the rasterization of the the shape file is greater than zero) and it is invaded by lava (i.e. its lava height is greater than zero). As shown in Figure 6a, the lava flow almost totally destroys the villages of Sarro Malopasso and Pisano, and a little bit of Fleri, getting an initial (no barriers) PSO score of 1737.

The algorithm proceeded following the PSO's logic until the score didn't get any improvements from one step to another in a fixed number of steps (i.e. 10).

Figure 6b shows the best configuration found, with a score equal to zero, which totally safeguards the villages of Sarro Malopasso, Pisano and Fleri, diverting the flows in uninhabited areas. Details about the location and geometric features of each barrier in the optimal configuration are reported in Table 1.

	easting	northing	langle	rangle	length	height
Barrier 1	506270	4169180	−90	−35	+191	+18
Barrier 2	506330	4169180	−84	−90	+68	+12
Barrier 3	505190	4170330	+90	−90	+256	+32
Barrier 4	504430	4171000	+71	+78	+256	−19
Barrier 5	507240	4168850	+90	+90	+39	−32
Barrier 6	504870	4170940	−90	+81	0	−32
Barrier 7	505290	4170530	−90	−15	+256	−32
Barrier 8	504450	4171030	+90	+6	0	+13
Barrier 9	505240	4170210	−8	+27	+180	−32

Table 1
Best particle configuration. For each barrier, the location and geometric characteristics (langle and rangle in degrees, length and height in meters) are reported.

Even if a maximum number of 9 barriers was set, the algorithm finds an optimal configuration using only 6 barriers. Indeed, barriers 6 and 8 have a null length and barrier 5 doesn't interact with the lava flow. Moreover the optimal

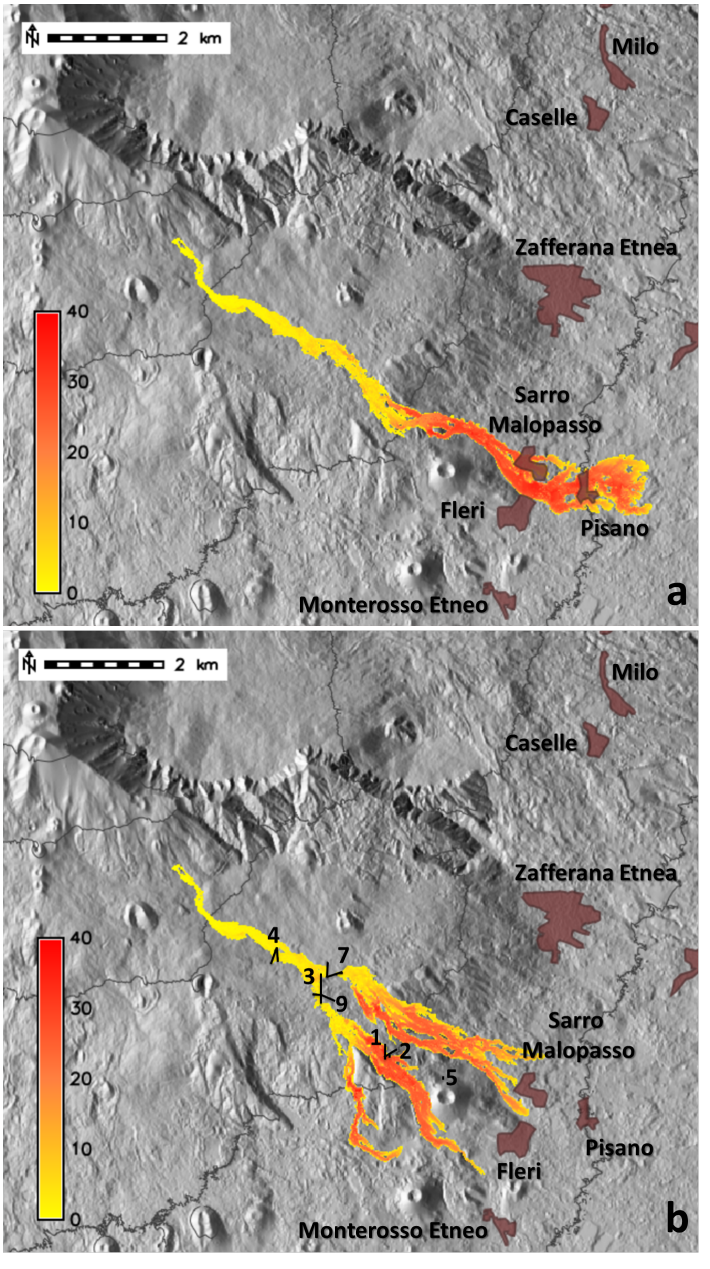

Figure 6: a) MAGFLOW simulation without any barriers, reaching a score of 1737; b) Best configuration obtained using our PSO approach, which brings the score to zero. Barriers are numbered as reported in Table 1. Barriers 6 and 8 are not displayed because their length is zero. Legends indicate the lava flow thickness in meters.

configuration shown in Figure 6b demonstrates that a combined use of both ditches (4, 7 and 9) and barriers (1, 2 and 3) can improve the results, leading to a total diversion of the lava flow to uninhabited zones.

6. Discussion

The results achieved by the combined use of the PSO approach and the numerical MAGFLOW model show the viability of this approach for the planning of mitigation actions to reduce the lava flow risk. With the given target function, the algorithm has found an optimal configuration that provides a minimum value for the score, equal to zero.

The optimal configuration includes both ditches and barriers, which effectively spare all townships in the area, ensuring that the lava flow reaches zones where there would be minimal loss.

It should be noted that the target function we are currently using does not have a unique global minimum point, or equivalently, there could be other potential barrier configurations that would still achieve a null score. The one we found is just one of them, and running the algorithm multiple times, starting from different (random) initial configurations will generally find a different optimal result, as shown in Appendix B, where we present two other different runs for the test case having different optimal barrier configurations.

This possible variability is partly intrinsic to the problem, and partly due to the specific choice of target function. Indeed, as we already mentioned previously, the current target function is "bare bones", considering only the township areas as meaningful losses. A more complete and realistic target function, which also considers scattered edifices and/or land use characteristics, would have a much smaller set of configurations, able to achieve a minimum value (probably larger than zero).

An additional aspect regards the cost of the interventions (emplacement of barriers, digging of tranches), that depends (among other things) on the position and size of the barriers (length and height). Adding to the target function the cost of the barrier itself would give additional constraints to the optimality of the solution, balancing the value gained by avoiding the loss from the lava flow with the cost of the intervention: the configuration would be then optimal in that it would be the least expensive solution to achieve the highest reduction of losses.

Another important point is is the computational performance of the algorithm. While computationally more intensive than a standard PSO due to the elaborations needed to enforce the constraints, the evolution of the swarm in our proposed methodology is not the most expensive part of the algorithm. Most of the computational time is spent instead in the evaluation of the target function. Since a MAGFLOW simulation is run for every particle in the swarm, a system with N particles will require $N \times S$ MAGFLOW simulations to complete S steps. For the test case on Etna, a single MAGFLOW run may take anywhere from 8 minutes to several hours, with the total run-time essentially dictated by the time-step, which in turn depends on the lava flow flux between cells. In particular, we observed that large accumulations of lava (such as in presence of a tall barrier or deep ditch) lead to a significant decrease in the time-step, and thus to longer simulations. While several hours to simulate 15 days of lava flow is an excellent time, when this needs to be multiplied by the number of particles to determine the computational run-time of a single step of the PSO, the computational time becomes a critical issue, suggesting it is important to reduce the computational time of a single MAGFLOW simulation, and/or find other ways to reduce the overall run-time or a single step, for example by simulating multiple particles concurrently.

7. Conclusions and future work

Lava flows are a form of volcanic phenomena that can cause significant social and economic losses on the inhabited areas and land use properties near the volcanoes. The growing use of these regions in the last decades led to an increasing demand for faster and effective methods for safeguarding population, properties, and services.

Lava flow risk maps constitute powerful instruments to evaluate the real cost of living in volcanic areas and provide valuable tools for the long-term planning of the territory (Del Negro et al., 2019). However, short-term mitigation measures are also needed for defense purposes to manage eruptive emergencies during volcanic crises. One of the most significant short-term measure to mitigate the destructive effects of lava flows is the building of artificial barriers or ditches in order to modify the path of the flows. This is a non trivial issue, as it requires to determine the correct position of each barrier following logistical placements limits, together with its best dimensions and geometries in order to minimize the damages caused by the flow and the intervention time.

We presented a new optimization algorithm based on PSO and the MAGFLOW numerical model for the simulation of lava flow paths, to determine the position and the geometric features of a barrier system that minimize the lava flow impact on properties and services.

The algorithm is divided in three phases. The first phase (pre-flight) runs a MAGFLOW simulation without barriers, to assess the initial conditions and compute the best score in absence of intervention. The next phase (particle system initialization) is the initialization of the particle system from the user-provided configuration (number of particles and their geometrical characteristics) and with random positions and velocities; the best initial score for each particle and for the whole swarm is computed by running a MAGFLOW simulation for each configuration given by the swarm. The last phase (swarm evolution) consists in the PSO swarm evolution following (1), modified to take into account the constraints that structures should interact with the flow and be at a certain distance from the vent and

from the towns. The particles' and swarm's best score get updated by running MAGFLOW simulations for each new configuration, and the phase gets repeated until convergence is reached (either the minimum possible score is achieved, or the score does not improve for a user-chosen number of steps).

The effectiveness of our methodology was validated over a destructive event possibly occurring on the south flank of Etna volcano. The hypothetical lava flow was supposed to totally overcome the villages of Sarro Malopasso and Pisano, and the northern part of Fleri. Our approach for the mitigation of lava flow risk provides an optimal barrier configuration that totally safeguarded these towns, diverting the flows in uninhabited zones. Moreover, the optimal configuration is made up of less mitigation structures (6) than the maximum one set by the user (9), and combines both barriers and ditches, demonstrating the effectiveness of their use. Although this study was carried out at Mt Etna, the approach used is designed to be applicable to any volcanic area where the input parameters needed by MAGFLOW and data about inhabited areas are available.

In this early stage, we have mainly dealt with the development and validation of our methodology, focusing on how to bridge the gap between the abstract aspects of PSO and the specific applications, and in particular on the minimization of the search space and the application of the constraints about barrier placement. With these issues now fixed, our future work will focus on overcoming the main limitation, that is the use of the original version of the particle swarm optimization algorithm and its susceptibility to be trapped in local minimal points. The problem of local minimum did not present in this initial phase, because the target function is discrete with an absolute minimum that is zero, but it may occur once we switch to a more refined target function that also takes into consideration scattered buildings and/or land use characteristics.

~~Our intent is to couple PSO with simulated annealing (SA), an approach already proposed for other applications, to integrate the merits of good exploration capability of PSO and the good local search properties of SA.~~

Our intent is to adopt a hybridization of PSO with some other methods that would help avoid local minimum trap, such as simulated annealing (Kirkpatrick et al., 1983; Černỳ, 1985), as done in e.g. S.Sudibyo et al. (2015), or the grey wolf optimizer (Mirjalili et al., 2014), as done in e.g. Singh and Singh (2017)).

Future work will also include a more thorough validation of the method with additional test cases, more realistic and feasible barriers' settings, and a sensitivity analysis of the model parameters.

The first step will be to include a complete urban scheme for the simulations, where beside cities, we will also take into consideration the land use properties and roads, with the potential legal disputes that could incur in diverting lava flows to sensitive areas. This can be done by giving each element a different value in the score calculation in PSO's logic, depending on its importance. This chance will probably prevent the score from ever dropping to zero, except if the eruptions is in totally uninhabited areas —in which case we are not interested in taking action. Even if the final score is non-zero, the PSO algorithm should allow us to provide a strategy to minimize (albeit not nullify) the damage caused by the flows.

The improvement to the target function will also include the attribution of an economic cost to each barrier configuration, so that we can expand the algorithm to minimize both the impact of lava flows on exposed elements and the cost of the construction of the systems. Coupled with an analysis of the financial losses due to the lava flow impact, this would provide further insights on the optimal intervention.

In order to improve the execution time, which is mostly entirely given by that of MAGFLOW simulation run for each particle configuration, we plan to parallelize our algorithm in such a way as to simulate more particles simultaneously, both by using more GPUs and by improving MAGFLOW to run multiple related scenarios at once.

With the refined target function and improved computational time, we will then have all the tools needed for a complete robustness and sensitivity analysis of the algorithm.

8. Acknowledgements

This work was developed within the framework of the Laboratory of Technologies for Volcanology (TechnoLab) at the INGV in Catania (Italy). The research was conducted in the framework of the research project "SHIELD – Optimization strategies for lava flow risk reduction at Etna volcano" (Bando di Ricerca Libera 2019 of INGV) and funded by the ATHOS Research Programme. We would like to thank the Editor-in-Chief Dan Ames for handling the paper, and the two anonymous referees for their suggestions that helped improving the clarity of the paper.

A. Enforcing the barrier position constraints

When defining or moving a barrier, certain zones have to be excluded from the space of configuration, because barriers cannot logically be too close to the vent position or inside the inhabited areas. Moreover, we want the barriers to interact with the flow, since otherwise their presence is unwarranted.

Consequently, when modifying barriers' position, the algorithm checks if the final position satisfies the constraints, and if this is not the case, it moves the barrier to a nearby location that satisfies them.

If the barrier is inside the vent exclusion region, the algorithm moves it outwards the minimum acceptable distance, m_d, which is set to 2km.

This is achieved by first computing the barrier/vent distance b_v, and if this is less than the m_d parameter, the barrier is moved to the point of intersection between the vent/barrier line and the circumference centered at the vent and with radius m_d: we add to the vent position a vector equal to the current vent/barrier vector, scaled by m_d/b_v (Figure 7). If the barrier happens to be very close to the vent, a random direction is chosen instead, to avoid numerical issues related to b_v being too small.

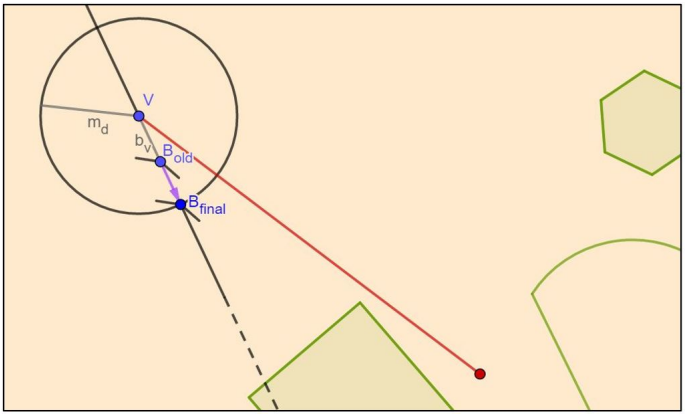

Figure 7: Representation of the procedure by which a barrier is pushed outside the vent exclusion region. In particular, the red line represents the lava flows, while the polygons in green represent the inhabited areas.

If the vent exclusion region intersects the boundary of the area of interest, the outwards push may move the barrier outside of the area of interest. In this case, the barrier position is corrected again by moving it to to the opposite edge of the vent exclusion (Figure 8).

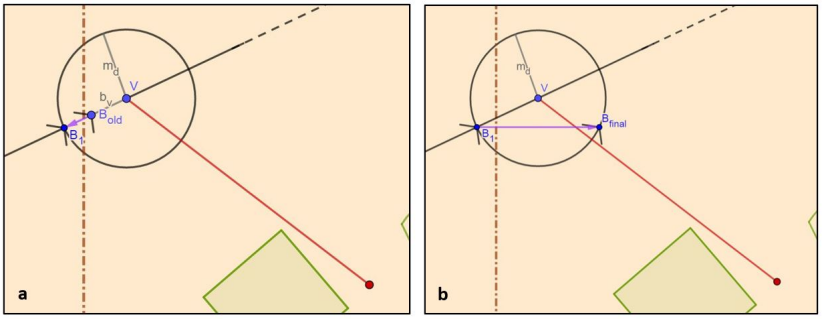

Figure 8: Representation of the barrier moving procedure in the case the vent exclusion region intersects the boundary of the research space(dashed/pointed line). The barrier is first pushed outside the vent exclusion area (a) and then, if outside the domain, it is moved to the opposite edge of the vent exclusion (b). In particular, the red line represents the lava flows, while the polygons in green represent the inhabited areas.

The next step is to verify that the barriers does not intersect an inhabited area. For each township within our area of interest, we compute the smallest circle that envelops the township's defining polygon and centered on the centroid of the same polygon: this defines the township's exclusion region.

If a barrier falls within a township's exclusion region, it is pushed outwards, towards the vent. Mathematically, this can be described as follows. Let C be the township's centroid and r the radius of the exclusion region. Then the boundary of the exclusion region is defined by the circle's equation:

$$\|x - C\|^2 = r^2. \tag{2}$$

If V is the vent position and B the barrier position, then the vent/barrier segment is described by the equation

$$x = B + t(V - B), \qquad t \in [0, 1]. \tag{3}$$

Since we are under the assumption that the barrier is inside the circle surrounding the inhabited area, its distance from the centroid is lower than the radius of the circle, i.e. the following inequality is verified:

$$\|B - C\|^2 < r^2. \tag{4}$$

To determine the intersection points between the circle and the barrier-vent straight line we replace the generic point $P(t) = B + t(V - B)$ of the straight line in the circle's equation (2), obtaining the following condition:

$$\|(B - C) + t(V - B)\|^2 = r^2,$$

or, equivalently

$$\|V - B\|^2 t^2 + 2\langle (B - C), (V - B)\rangle t + \|B - C\|^2 - r^2 = 0 \tag{5}$$

where $\langle \cdot, \cdot \rangle$ represents the dot product.

Equation (5) is a quadratic equation in the unknown t which, due to the geometry of our points, admits two distinct real solutions. We want the solution in the range $[0, 1]$, since this would represent the intersection point between the segment (3) and the circle (2). To find the solution, we calculate the discriminant:

$$\frac{\Delta}{4} = \langle (B - C), (V - B)\rangle^2 - \|V - B\|^2(\|B - C\|^2 - r^2),$$

and we know that, because of (4), it is non-negative.

Therefore, the two solutions of equation (5) are:

$$t_1 = -\frac{\langle (B - C), (V - B)\rangle - \sqrt{\Delta/4}}{\|V - B\|^2}, \quad t_2 = -\frac{\langle (B - C), (V - B)\rangle + \sqrt{\Delta/4}}{\|V - B\|^2}.$$

The new barrier position is then obtained substituting the solution of (5) withing the range $[0, 1]$ in equation (3).

Finally, since we want to ensure that the barrier interacts with the flow, we move the barrier position to the nearest point of the lava flow (Figure 9).

Since the flow associated to the new configuration is not know yet, the flow/barrier distance is computed according to the flow emplacement obtained for the PSO particle at the last step (in the case of the first step, we consider instead the flow emplacement without any barriers).

Specifically, the results of the MAGFLOW simulation for each particle are imported, cutting out the flow areas that intersect the vent and townships' exclusion regions. Then for each barrier in the particle, we compute the position update according to the PSO algorithm, apply the barrier shifting due to the vent and township exclusion regions (if necessary), and finally compute the distance between the shifted barrier position to each DEM cell occupied by lava (according to the particle's previous configuration) and move the barrier to the coordinates of the closest cell.

According to the quantization of the dimensions discussed in section 4.2, each of the corrections applied during the constraint procedure is done by rounding up the position displacement vector to the next multiple of the position quantization step.

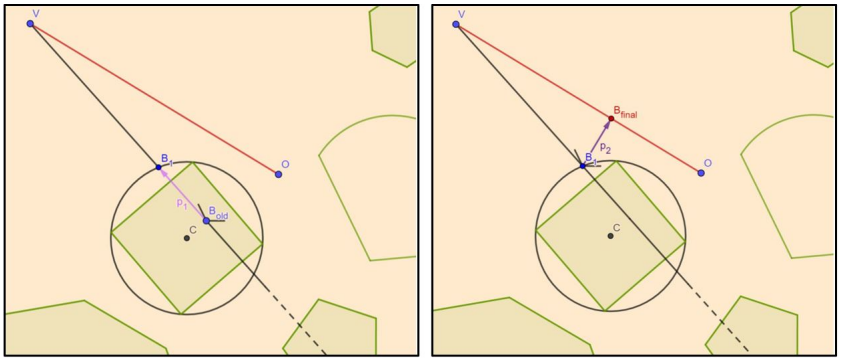

Figure 9: Representation of the procedure by which a barrier is first pushed outside the inhabited area (on the left) and then snapped to the lava flow (on the right). Note that the snap-to-flow is done also if the barrier wasn't originally within a township exclusion region.

B. Results of other runs for the test case

We present other two runs, named as run *A* and run *B*, for the test case presented in Section 5 to validate our PSO–based algorithm. We aim to show the non-unique global minimum point of the target function currently used, which is the potential loss associated with an eruptive scenario where the loss, in this initial stage of development, is defined by simply estimating the amount of inhabited areas reached by the lava flow. As we already pointed up, the fact that there could be other potential barrier configurations that still achieve a null score, i.e. no inhabited area is inundated, is mainly due to our early-stage definition of the target function. In the future we plan to extend it to be more complete and realistic for the assessment of lava flow risk, considering also scattered edifices and/or land use characteristics. This would probably lead to having a minimum value larger than zero, reached by a smaller set of configurations.

Figures 10 and 11 show the best configuration found by run *A* and run *B* of our algorithm, with almost the same specifications of the test case starting from different (random) initial configurations. The only different value is the suitable maximum number of barriers that we decide to decrease by one unit (thus it is 8), since the optimal configuration found in the test case used only 6 barriers compered with the 9 maximum fixed.

As expected, the results obtained show different optimal result with respect to 5, presenting other potential barrier configurations that still achieve a null score, totally safeguarding the threatened villages of Sarro Malopasso, Pisano, and Fleri, diverting the flows in uninhabited areas.

Tables 2 and 3 report details about the location and geometric features of each barrier in the optimal configuration of the two runs.

We can see how in run *A* even if a maximum number of 8 barriers was set, the algorithm finds an optimal configuration using again only 6 barriers. Indeed, barriers 6 and 7 don't interact with the lava flow (10). Moreover, also the optimal configuration of run *A* includes both ditches (1, 3, and 4) and barriers (2, 5, and 8).

	easting	northing	langle	rangle	length	height
Barrier 1	505150	4170690	−87	+4	256	−32
Barrier 2	507980	4169220	+90	−90	168	11
Barrier 3	505090	4170280	+90	−90	256	−32
Barrier 4	507050	4169480	+90	+90	163	−32
Barrier 5	507670	4169060	+60	−90	256	+23
Barrier 6	509150	4168270	−20	−90	120	+7
Barrier 7	509190	4168250	−90	+90	69	−11
Barrier 8	508080	4169160	−51	+90	181	+32

Table 2
Best particle configuration of run *A*. For each barrier, the location and geometric characteristics (langle and rangle in degrees, length and height in meters) are reported.

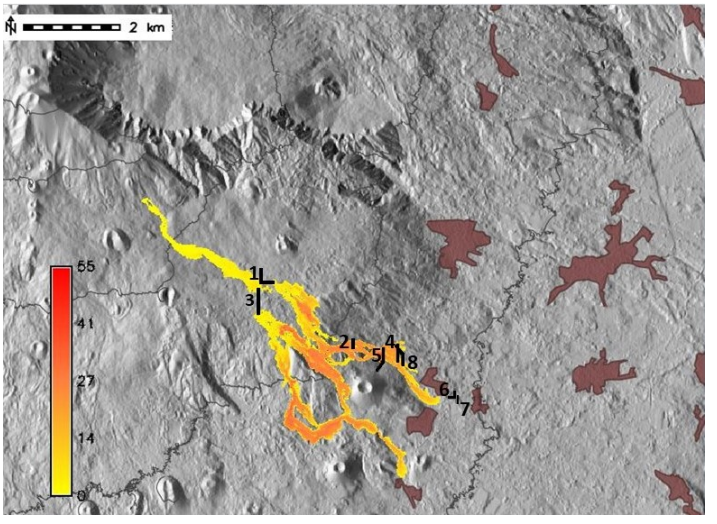

Figure 10: Best configuration for run *A* obtained using our PSO approach, which brings the score to zero. Barriers are numbered as reported in Table 2. Legends indicate the lava flow thickness in meters.

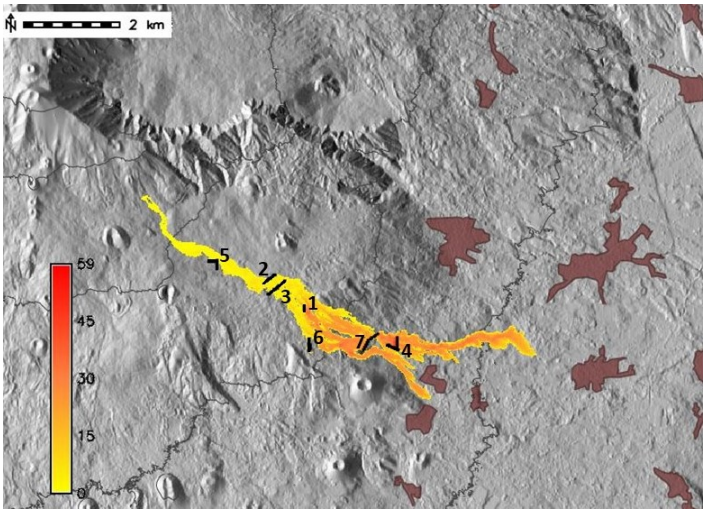

Figure 11: Best configuration of run *B* obtained using our PSO approach, which brings the score to zero. Barriers are numbered as reported in Table 3. Barrier 8 is not displayed because its length is zero. Legends indicate the lava flow thickness in meters.

In run *B* the algorithm finds an optimal configuration using only 7 barriers, even if a maximum number of 8 barriers was set, having barrier 8 a null length. Moreover, the optimal configuration shown in Figure 11 demonstrates how once again the combined use of both ditches (2, and 7) and barriers (1, 3, 4, 5, and 6) can improve the results, leading to a total diversion of the lava flow to uninhabited zones.

	easting	northing	langle	rangle	length	height
Barrier 1	506050	4170090	−89	+88	41	+23
Barrier 2	505340	4170710	+41	−35	115	−22
Barrier 3	505480	4170510	+38	−41	219	+6
Barrier 4	507980	4169220	−29	−90	259	+23
Barrier 5	504250	4171070	+9	+88	165	+32
Barrier 6	506150	4169470	+90	+82	256	+32
Barrier 7	507380	4169430	+63	−34	226	−32
Barrier 8	510210	4168770	−90	+44	0	−14

Table 3
Best particle configuration of run B. For each barrier, the location and geometric characteristics (langle and rangle in degrees, length and height in meters) are reported.

References

Andronico, D., Branca, S., Calvari, S., Burton, M., Caltabiano, T., Corsaro, R.A., Del Carlo, P., Garfi, G., Lodato, L., Miraglia, L., Muré, F., Neri, M., Pecora, E., Pompilio, M., Salerno, G., Spampinato, L., 2005. A multi-disciplinary study of the 2002–03 etna eruption: insights into a complex plumbing system. Bulletin of Volcanology 67, 314–330.

Barberi, F., Brondi, F., Carapezza, M., Cavarra, L., Murgia, C., 2003. Earthen barriers to control lava flows in the 2001 eruption of mt. etna. Journal of Volcanology and Geothermal Research 123, 231–243. doi:10.1016/S0377-0273(03)00038-6.

Barberi, F., Carapezza, M., 2004. The control of lava flow at mt. etna. Mt. Etna: Volcano Laboratory, Geophysical Monograph Series .

Barberi, F., Carapezza, M., Valenza, M., Villari, L., 1993. The control of lava flow during the 1991–1992 eruption of mt. etna. Journal of Volcanology and Geothermal Research 56, 1 – 34. doi:https://doi.org/10.1016/0377-0273(93)90048-V.

Behncke, B., Neri, M., Nagay, A., 2005. Lava flow hazard at Mount Etna (Italy): New data from a GIS-based study. volume 396. pp. 189–208. doi:10.1130/0-8137-2396-5.189.

Bilotta, G., Cappello, A., Hérault, A., Del Negro, C., 2019. Influence of topographic data uncertainties and model resolution on the numerical simulation of lava flows. Environmental Modelling & Software 112, 1 – 15. doi:https://doi.org/10.1016/j.envsoft.2018.11.001.

Bilotta, G., Cappello, A., Hérault, A., Vicari, A., Russo, G., Negro, C.D., 2012. Sensitivity analysis of the magflow cellular automaton model for lava flow simulation. Environmental Modelling & Software 35, 122 – 131. doi:https://doi.org/10.1016/j.envsoft.2012.02.015.

Bonaccorso, A., Bonforte, A., Calvari, S., Del Negro, C., Di Grazia, G., Ganci, G., Neri, M., Vicari, A., Boschi, E., 2011. The initial phases of the 2008–2009 mount etna eruption: A multidisciplinary approach for hazard assessment. Journal of Geophysical Research: Solid Earth 116. doi:10.1029/2010JB007906.

Branca, S., Coltelli, M., Groppelli, G., Lentini, F., 2011. Geological map of etna volcano, 1:50,000 scale. Italian Journal of Geosciences 130, 265–291. doi:10.3301/IJG.2011.15.

Calvari, S., Pinkerton, H., 1998. Formation of lava tubes and extensive flow field during the 1991-1993 eruption of mount etna. Journal of Geophysical Research , 291–27doi:10.1029/97JB03388.

Calvari, S., Pinkerton, H., 1999. Lava tube morphology on etna and evidence for lava flow emplacement mechanisms. Journal of Volcanology and Geothermal Research 90, 263–280. doi:10.1016/S0377-0273(99)00024-4.

Cappello, A., Bilotta, G., Neri, M., Del Negro, C., 2013. Probabilistic modeling of future volcanic eruptions at mount etna. Journal of Geophysical Research: Solid Earth 118, 1925–1935. doi:10.1002/jgrb.50190.

Cappello, A., Hérault, A., Bilotta, G., Ganci, G., Del Negro, C., 2016. Magflow: A physics-based model for the dynamics of lava-flow emplacement. Geological Society, London, Special Publications 426. doi:10.1144/SP426.16.

Černỳ, V., 1985. Thermodynamical approach to the traveling salesman problem: An efficient simulation algorithm. Journal of optimization theory and applications 45, 41–51.

Colombrita, R., 1984. Methodology for the construction of earth barriers to divert lava flows: the mt. etna 1983 eruption. Bulletin Volcanologique 47, 1009–1038.

Del Negro, C., Cappello, A., Bilotta, G., Ganci, G., Hérault, A., Zago, V., 2019. Living at the edge of an active volcano: Risk from lava flows on Mt. Etna. GSA Bulletin 132, 1615–1625. doi:10.1130/B35290.1.

Del Negro, C., Cappello, A., Neri, M., Bilotta, G., Hérault, A., Ganci, G., 2013. Lava flow hazards at mount etna: constraints imposed by eruptive history and numerical simulations. Scientific Reports 3. doi:10.1038/srep03493.

Del Negro, C., Fortuna, L., Hérault, A., Vicari, A., 2008. Simulations of the 2004 lava flow at etna volcano using the magflow cellular automata model. Bulletin of Volcanology 70, 805–812. doi:10.1007/s00445-007-0168-8.

Dorigo, M., 1992. Optimization, learning and natural algorithms. Ph.D. Thesis .

El-Ghandour, H., Elbeltagi, E., 2018. Comparison of five evolutionary algorithms for optimization of water distribution networks. Journal of Computing in Civil Engineering 32, 04017066. doi:10.1061/(ASCE)CP.1943-5487.0000717.

Favalli, M., Tarquini, S., Fornaciai, A., Boschi, E., 2009. A new approach to risk assessment of lava flow at mount etna. Geology 37, 1111–1114. doi:10.1130/G30187A.1.

Filippone, G., Spataro, W., D'Ambrosio, D., Marocco, D., 2013. A new methodology for mitigation of lava flow invasion hazard: Morphological evolutionof protective works by parallel genetic algorithms, in: IJCCI 2013 - Proceedings of the 5th International Joint Conference on Computational Intelligence.

Fournier D'Albe, E.M., 1979. Objectives of volcanic monitoring and prediction. Journal of the Geological Society 136, 321–326. doi:10.1144/gsjgs.136.3.0321.

Ganci, G., Vicari, A., Cappello, A., Del Negro, C., 2012. An emergent strategy for volcano hazard assessment: From thermal satellite monitoring to lava flow modeling. Remote Sensing of Environment 119, 197–207. doi:10.1016/j.rse.2011.12.021.

Glover, F., Marti, R., 2006. Tabu Search. Springer US, Boston, MA. pp. 53–69. URL: https://doi.org/10.1007/0-387-33416-5_3, doi:10.1007/0-387-33416-5_3.

Gogna, A., Tayal, A., 2013. Metaheuristics: review and application. Journal of Experimental & Theoretical Artificial Intelligence 25, 503–526. doi:10.1080/0952813X.2013.782347.

Holland, J.H., 1992. Adaptation in Natural and Artificial Systems: An Introductory Analysis with Applications to Biology, Control and Artificial Intelligence. MIT Press, Cambridge, MA, USA.

Hérault, A., Vicari, A., Ciraudo, A., Del Negro, C., 2009. Forecasting lava flow hazards during the 2006 etna eruption: Using the magflow cellular automata model. Computers & Geosciences 35, 1050–1060. doi:10.1016/j.cageo.2007.10.008.

Kennedy, J., Eberhart, R., 1995a. A new optimizer using particle swarm theory, in: MHS'95. Proceedings of the Sixth International Symposium on Micro Machine and Human Science, pp. 39–43.

Kennedy, J., Eberhart, R., 1995b. Particle swarm optimization, in: Proceedings of ICNN'95 - International Conference on Neural Networks, pp. 1942–1948.

Kirkpatrick, S., Gelatt, C., Vecchi, M., 1983. Optimization by simulated annealing. Science (New York, N.Y.) 220, 671–80. doi:10.1126/science.220.4598.671.

Mirjalili, S., Mirjalili, S.M., Lewis, A., 2014. Grey wolf optimizer. Advances in Engineering Software 69, 46–61. URL: https://www.sciencedirect.com/science/article/pii/S0965997813001853, doi:https://doi.org/10.1016/j.advengsoft.2013.12.007.

Pedrazzi, D., Cappello, A., Zanon, V., Del Negro, C., 2014. Impact of effusive eruptions from the eguas - carvão fissure system, são miguel island, azores archipelago (portugal). Journal of Volcanology and Geothermal Research doi:10.1016/j.jvolgeores.2014.12.012.

Price, K., Storn, R.M., Lampinen, J.A., 2005. Differential Evolution: A Practical Approach to Global Optimization (Natural Computing Series). Springer-Verlag, Berlin, Heidelberg.

Scifoni, S., Coltelli, M., Marsella, M., Proietti, C., Napoleoni, Q., Vicari, A., Del Negro, C., 2010. Mitigation of lava flow invasion hazard through optimized barrier configuration aided by numerical simulation: The case of the 2001 etna eruption. Journal of Volcanology and Geothermal Research 192, 16 – 26. doi:https://doi.org/10.1016/j.jvolgeores.2010.02.002.

Shi, Y., Eberhart, R., 1998. A modified particle swarm optimizer, in: 1998 IEEE International Conference on Evolutionary Computation Proceedings. IEEE World Congress on Computational Intelligence (Cat. No.98TH8360), pp. 69–73.

Singh, N., Singh, S.B., 2017. Hybrid algorithm of particle swarm optimization and grey wolf optimizer for improving convergence performance. Journal of Applied Mathematics 2017. doi:https://doi.org/10.1155/2017/2030489.

S.Sudibyo, M.N.Murat, N.Aziz, 2015. Simulated annealing-particle swarm optimization (sa-pso): Particle distribution study and application in neural wiener-based nmpc, in: 2015 10th Asian Control Conference (ASCC), pp. 1–6. doi:10.1109/ASCC.2015.7244567.

Thierry, P., Stieltjes, L., Kouokam, E., Nguéya, P., Salley, P., 2008. Multi-hazard risk mapping and assessment on an active volcano: The grinp project at mount cameroon. Natural Hazards 45, 429–456. doi:10.1007/s11069-007-9177-3.

Vicari, A., Ciraudo, A., Negro, C.D., Herault, A., Fortuna, L., 2009. Lava flow simulations using discharge rates from thermal infrared satellite imagery during the 2006 etna eruption. Natural Hazards: Journal of the International Society for the Prevention and Mitigation of Natural Hazards 50, 539–550. doi:10.1007/s11069-008-9306-7.

Vicari, A., Ganci, G., Behncke, B., Cappello, A., Neri, M., Del Negro, C., 2011. Near-real-time forecasting of lava flow hazards during the 12–13 january 2011 etna eruption. Geophysical Research Letters 38. doi:10.1029/2011GL047545.

Vicari, A., Hérault, A., Del Negro, C., Coltelli, M., Marsella, M., Proietti, C., 2007. Modeling of the 2001 lava flow at etna volcano by a cellular automata approach. Environmental Modelling & Software 22, 1465 – 1471. doi:https://doi.org/10.1016/j.envsoft.2006.10.005.

Walker, G.P.L., Guest, J.E., Skelhorn, R.R., 1973. Mount etna and the 1971 eruption - lengths of lava flows. Philosophical Transactions of the Royal Society of London. Series A, Mathematical and Physical Sciences 274, 107–118. doi:10.1098/rsta.1973.0030.